Effects of background rotation on a towed-sphere wake in a stably stratified fluid (*)(**)

G. R. SPEDDING (1)(***) and A. M. FINCHAM (2)

(1) *Department of Aerospace and Mechanical Engineering, University of Southern California Los Angeles, USA*
(2) *Laboratoire Coriolis, Institut de Méchanique de Grenoble, France*

(ricevuto il 18 Novembre 1998; approvato il 6 Maggio 1999)

Summary. — The wake of a towed sphere in a stable background density gradient can be considered a convenient model problem for studying the emergence and longevity of the coherent patches of alternate-signed vertical vorticity that comprise the late wake. In practical applications it is likely that the lifetime is such that rotation effects should also be considered, and strong rotation can also be used to deliberately disturb the inferred three-dimensional wake structure. Competing effects of stratification and rotation can be measured by the ratio of rotation to buoyancy timescales, f/N, which varies from 0.05 to 0.22 in experiments conducted on the 14 m diameter rotating table at Coriolis. Wake anticyclones, with sense of rotation opposite to the background rotation, were spread out over a larger area, and were less strongly peaked than their cyclonic counterparts, with the magnitude of the asymmetry depending on f/N. Deformation of anticyclones into highly elliptical shapes coincided with a broader range of wake vortex interactions than in the non-rotating case. At much longer times (hundreds of buoyancy periods, 5-10 rotation times), a recircularisation of elliptical anticyclones can occur. The observed asymmetries are consistent with existing data on homogeneous wake flows with rotation.

PACS 92.10.Ei – Coriolis effects.
PACS 92.10.Lq – Turbulence and diffusion.
PACS 47.55.Hd – Stratified flows.
PACS 47.27.Vf – Wakes.
PACS 01.30.Cc – Conference proceedings.

1. – Residual vortex motions from initially turbulent flows

The propensity for various geophysical flows over a range of length scales to culminate in the generation of a relatively small number of coherent vortex structures

(*) Paper presented at the International Workshop on "Vortex Dynamics in Geophysical Flows", Castro Marina (LE), Italy, 22-26 June 1998.
(**) The authors of this paper have agreed to not receive the proofs for correction.
(***) Experiments conducted while GRS held post of *Stagiaire* at IMG, Grenoble.

has been noted many times. In a recent review, Lighthill [1] noted how, following a small, local disturbance in a uniform stratification, the fluid motions remaining after internal waves have propagated away are steady, with no variation in 2D planar motion, or in the vertical shearing between horizontal layers. Both horizontal and vertical components of vorticity persist and particular topologies of closed vortex lines do not change. The time-invariant vertical vorticity mode was first described by the small Froude number scaling analysis of Riley *et al.* [2], and these ideas have found quite broad application to late-time evolution of initially turbulent flows. A further characteristic of stably stratified flows is that information concerning the generating conditions can be preserved and will be felt in the structure of the vortex patches that comprise the "residual" velocity field. Hence, in the laboratory, fluid ejected from an orifice usually generates a dipole, *e.g.* [3-5], and numerical simulations confirm that laminar jets or turbulent patches with some net linear momentum are sufficient for dipole emergence [6, 7]. Swirling motion frequently generates a monopole [8, 9], and separated flow over a flat plate or bluff body generates an array of opposite-signed, coupled vortex patches, *e.g.*, [10-12]. In the field, characteristic vortex structures can be produced repeatedly near certain topographies, and once generated, lifetimes are measured in weeks and months. It is of some interest to know how, and which information from the initial conditions survives in the late-time flow.

1·1. *Particular and general characteristics of towed-sphere wakes.* – The towed sphere is thus one instance of a rather broad class of flows that can generate long-lived, stable vortex structures from turbulent initial conditions. The comparative importance of the inertial forces relative to the restoring buoyancy force in a uniform density gradient is measured by the internal Froude number, $\mathrm{Fr} = 2U/ND$, based on the body speed, U, and radius, $D/2$, where the buoyancy frequency, $N = (-g/\varrho_0(\partial\varrho/\partial z))^{1/2}$ is constant. In the turbulent sphere wake, Fr measures the ratio of turbulence convective timescales to internal oscillatory timescales, and when Fr is large, the turbulence might be expected to disorganise the fluid motions to such an extent that any regularity imposed by the body geometry or motion is lost. However, this notion is contradicted by experimental findings [13] where persistent vortex wakes were measured for values of Fr up to 240, with no sign of a strong dependence on Fr in the long-time structure or longevity. The most reasonable extrapolation of this result is that all stratified wakes will behave this way, at any finite Fr.

The particular regularity that is preserved in the late wake of the towed sphere appears to derive from the spiral mode shedding at the sphere surface. The way in which the early 3D turbulence transitions through a non-equilibrium phase of readjustment to quasi–two-dimensional (Q2D) dynamics however is argued to be quite general. Decreased energy density decay rates close to the origin of the disturbance are attributable to reconversion of potential energy of fluid displaced from its equilibrium density level. The readjustment occurs when local Froude numbers have a value of 1, and the physical mechanism is general for a decaying flow in a stable, uniform, background density gradient. Once established, the late-time flow has negligible vertical velocity (parallel to the density gradient), and the Q2D velocity fields at each level proceed quite independent of the ambient density field. The late-time Fr-independence is thus unsurprising.

1·2. *Anticipated effects of rotation.* – If wake lifetimes of $Nt \approx 10^3$ are expected (regardless of Fr), $N \approx 10^{-3}$ close to the ocean pycnocline, then $t \approx 10^6$, which is about

10 Earth rotation periods. Choosing a characteristic velocity scale, u as the mean wake centreline velocity, and a characteristic length scale, l, as the mean wake half-width in the horizontal, predicted values from scaling relationships for $(u/U)(Nt)$ and $(l/D)(Nt)$ in [12] and [13] lead to values of a local Rossby number defined as $\mathrm{Ro}_{\mathrm{loc}} = u/2\Omega l$ of approximately 0.2 when $Nt = 10^3$. After one day, $\mathrm{Ro}_{\mathrm{loc}} \approx 0.5$, and by the usual criterion for $\mathrm{Ro} < 1$, rotation could be of practical significance.

It has been conjectured [12] that the observed stability of the wake topology might be related to certain preferred spatial arrangements of vortex patches in the vertical direction. The well-known isotropising effects in the vertical of strong rotation (cf. [14, 15] for contrary effects in very fine-grained numerical simulations of decaying quasi-geostrophic turbulence) may enforce a rearrangement of vortex lines in the wake, whose measured effects might provide indirect evidence for the original, postulated topology.

2. – Experiments

2·1. *Procedure.* – Experiments were conducted in the 14 m diameter rotating table at the Coriolis facility, IMG, Grenoble (see [16, 17] for details). The tank was filled, at rest, with a continuously varying density salt solution by an inverted version of the traditional two-tank method, filling from the bottom first with light fluid. The tank was spun up with constant angular acceleration from rest over a 12 hour period and experiments began 36 or more hours after a constant angular velocity had been reached. Measured ambient energy and vorticity magnitudes decreased by two, and three orders of magnitude, respectively, during this period. Rotation periods, $T = 500$, 250, 150 and 125 s give angular rotations in the range $\Omega \in [0.013, 0.05]$ rad/s. Spheres of 9.7, 7.5 and 5.0 cm diameter were towed along a 6.1 m straight line track tangent to the tank arc at its central point. The spheres were located at a height, $h = 60$ cm from the bottom of the tank, in a water depth, $H = 1$ m.

Neutrally buoyant particles of polystyrene seeded the fluid about mid tank height, where measurements were made. Illumination was provided by a 5W Argon laser with fibre-optic coupling to a scanning mirror that was traversed across a large, underwater, 45 degree-inclined mirror. In passing through the fluid, the sheet describes a parabola, and the initial entry angle was adjusted so that the measurement area was centred on the top of the parabola. Maximum deviations of the light sheet from horizontal were a small fraction of the sphere diameter.

4-frame bursts were imaged onto a Pulnix TM9701 CCD (768×484) camera with digital interface. Each burst comprises one timestep, and most experiments were recorded for 100 timesteps over 20 minutes, with a linear increase in effective exposure time and inter-timestep delay over this period. The camera centre was 3.1 m from the sphere starting point, which is $30\text{–}60D$. All elapsed times were set to an origin when the sphere passed this centre point. Residual, background velocity fields varied in magnitude and structure with the rotation speed, and were checked and measured before each run, which began only when the maximum ambient flow speed was $1\text{–}5 \times 10^{-2}$ cm/s. The minimum time between runs was 3 hours at rest, and 4 hours for $T = 125$ s.

2·2. *Data analysis.* – Data were both recorded on, and processed by various networked PCs, using the CIV algorithms described in [18]. The 4-frame burst allows the effective exposure time to be carefully selected *a posteriori* from 6 possible values.

Given a certain physical setup (lighting, particles), it is the *only* experimental variable that subsequently affects the accuracy and bandwidth of the velocity estimates (and their spatial gradients). In each run, the interpolated residual velocity field was subtracted from each timestep. This correction, which is in any case small, assumes that the ambient disturbance timescales are long compared to the runtime, and that the flow field of interest is simply superimposed upon the background kinematics, having no effect on the dynamics.

The general wake analysis procedures for calculating mean wake dimensions and statistics are as originally documented in [19, 12]. The procedure for fitting elliptical Gaussian functions to, and tracking vortex patches in time is also given in [12].

3. – Results

In the non-rotating case, the dimensionless parameters are Fr and Re. In the rotating case, the Rossby number is $\mathrm{Ro} = U/fD$, where $f = 2\Omega$ is the Coriolis parameter, and initial values range from 200 to 7. The Ekman number, $\mathrm{Ek} = \nu/fH^2$, is always small, from 6 to 1.6×10^{-5}. The Burger number for this geometry can be defined as $S = N^2H^2/f^2D^2$, and is always large, with minimum value ≈ 1400. For small, and fixed D/H, the ratio f/N is the most convenient measure of the ratio of buoyancy to Coriolis timescales (for vertical scales of motion, D, with density difference $\Delta\varrho(D/H)$ on that scale, S reduces to f/N), and it varies from 3.6 at the slowest rotation rates to 0.2 at the fastest. In this short paper, only Re, Fr, Ro and f/N need be considered.

3·1. *Modified vertical vorticity distributions.* – Figure 1 shows the time evolution of the vertical component of vorticity

$$\omega_z = \frac{\partial v}{\partial x} - \frac{\partial u}{\partial y},$$

for $23 \leqslant Nt \leqslant 392$ at intervals of approximately $24Nt$, or about 4 buoyancy periods. The body passed from left to right through the camera frame of reference which rotates with the tank. The quasi-regular, and persistent vortex wake pattern is clearly established for $\mathrm{Ro} = 27$, $\mathrm{Fr} = 2.3$ and $\mathrm{Re} = 5 \times 10^3$. At this Re, moderate variations in Re are comparatively unimportant, and one looks at the ratio of Fr: $\mathrm{Ro} \sim f/N = 0.05$. Buoyancy forces are strong compared to the Coriolis force, and the usual wake geometry can can be expected to form well before rotation effects are felt. An elapsed time of one rotation period occurs at the middle of the third line in fig. 1. Nevertheless, careful inspection reveals apparent differences in the area occupied by blue anticyclones and yellow cyclones. The difference can be made more quantitatively, but for the present, it is sufficient to note that the qualitative asymmetry is first observable from quite early on—perhaps the second frame, where $Nt = 48$.

In fig. 2, a similar time series is shown for the case $\mathrm{Ro} = 27$, $\mathrm{Fr} = 18$ and $\mathrm{Re} = 10 \times 10^3$. The ratio of Fr to Ro has changed by a factor of 4 ($f/N = 0.22$), and the wake asymmetry is increasingly evident. At all times, the regions of cyclonic vorticity are more compact, and the pairing rate and departure from circular geometry are increased in the anticyclones. From frame # 2 to frame # 8, the increased pairing rate of the anticyclones leads to unequal numbers of positive- and negative-signed patches of $\omega_z(x, y)$, a local 2-anticyclone : 1-cyclone geometry being common. During this time,

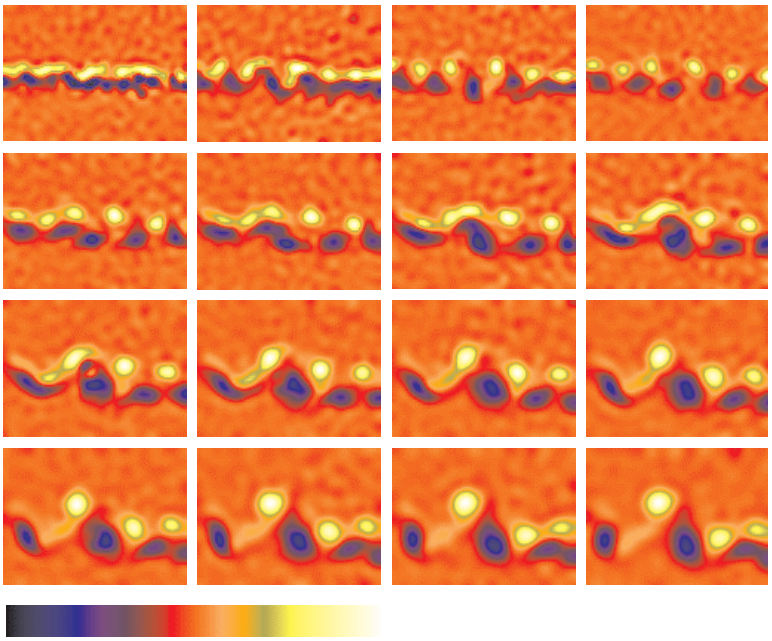

Fig. 1. – $\omega_z(x, y, Nt)$ for 16 approximately equally spaced time intervals $Nt = 23$–392. At $Nt = 0$, the body was at the centre of the observation box, moving from left to right. The observation box size is 208×152 cm. Fr $= 2.3$, Ro $= 27$, $f/N = 0.05$.

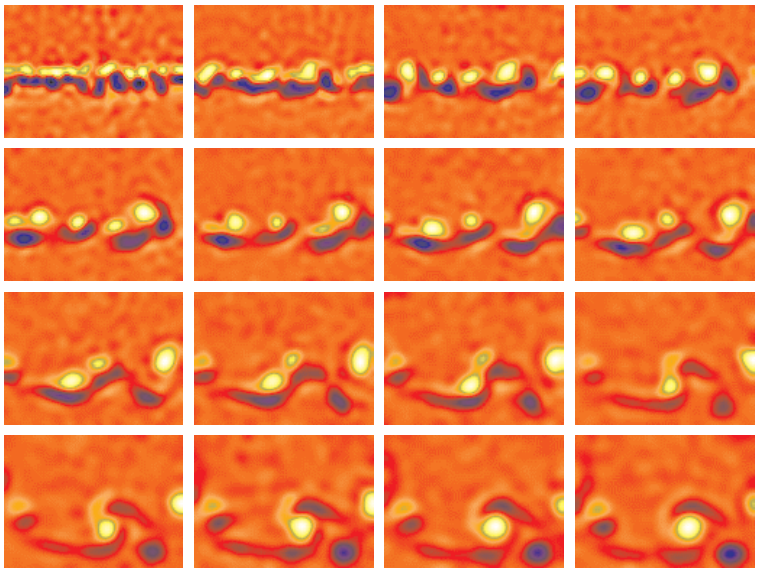

Fig. 2. – As fig. 1, but for Fr $= 18$, Ro $= 27$, $f/N = 0.22$. Nt ranges from 13 to 428 at timesteps of approximately $28\,Nt$, or 4.5 buoyancy periods. Each row covers about two rotations of the tank.

the cyclones have a compact, circular form. The range of vortex-vortex interactions in the wake is much more varied than in the absence of rotation, and in the last frame, $Nt = 428$, a tripolar structure has been formed and has remained in view over the entire bottom row, which is about 2 rotation periods and 18 buoyancy periods.

3·2. *Quantitative measures of wake asymmetry.* – Some brief examples of more quantitative measures of the wake asymmetry will be given.

Figure 3a compares the magnitude of the total circulation integrated over positive and negative vortex patches over the wake, as defined by the mean, local wake profile width [12] for the case Ro = 25, Fr = 8.6 and $f/N = 0.17$. The values for the positive and negative sides of the wake do not differ significantly. To a degree, this is reassuring, as the original shedding and production is symmetric. If the total circulation is unchanged then anticyclones occupying a comparatively larger area may be weaker than their cyclone counterparts, and fig. 3b shows this to be the case. After about $40\,Nt$, or $2\,T/3$, a significant asymmetry has developed in the maximum absolute vorticity magnitude, $|\omega_z|_{\max}$. This asymmetry persists for the length of the experiment.

The properties of individual vortex patches can be measured to understand their contribution to the statistical measures of fig. 3. Single patches were selected at late times and their time history reconstructed by stepping backwards through the time series. Figure 4 shows the result for two vortex patches of each sign for the same data as fig. 2, where $f/N = 0.22$. The ratio of major-to-minor axis length of each patch, a/b is plotted separately for the cyclones and anticyclones. The cyclones (fig. 4a) are almost circular, or close to it, and departures can be associated with pairing or other local

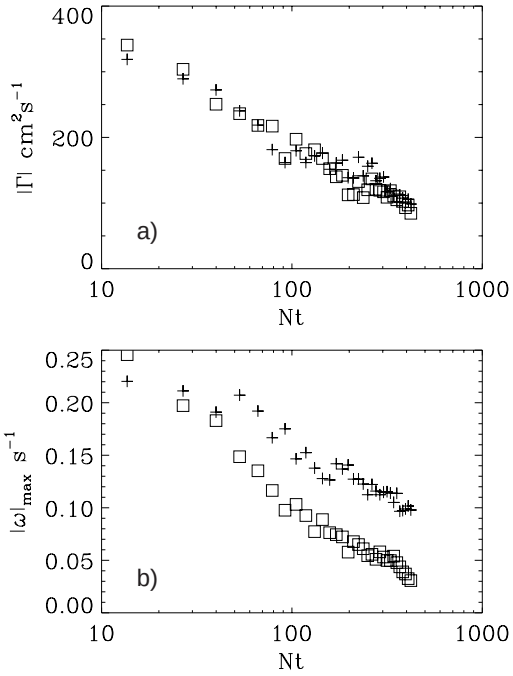

Fig. 3. – a) The absolute value of the total circulation for cyclones (+) and anticyclones (□) in the wake for Ro = 25, Fr = 8.6 and $f/N = 0.17$. b) The maximum vorticity magnitude for the same data.

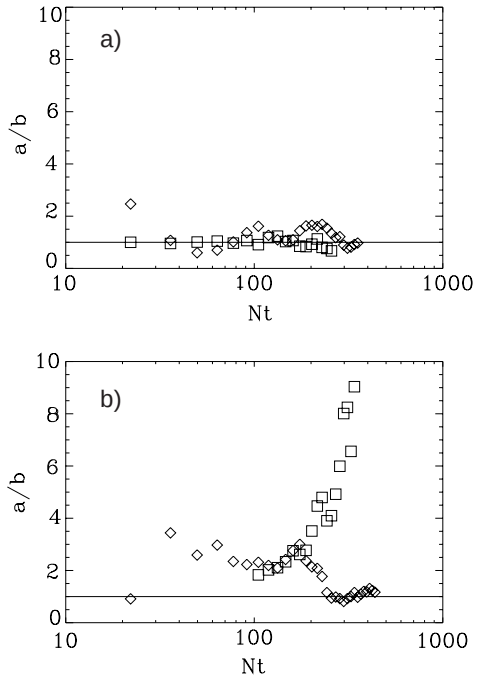

Fig. 4. – The aspect ratio a/b of two selected cyclones (a), and two anticyclones (b) for the experiment in fig. 2. The major and minor axes lengths are calculated from least-squares fits of elliptic Gaussian functions.

interactions. The anticyclones are non-circular for most of their lifetime. At late times, the aspect ratio can become very high, or a return to circularity may be observed.

4. – The effects of stratification and rotation

The effect of background rotation is to generate an asymmetry in the wake, where the anticyclonic vortex cores are more irregular in structure and spread over a broader area. Conversely, cyclones become more compact, and have strongly peaked cores. At high rotation rates, the early wake is modified, with highly three-dimensional motion occurring in the regions that will eventually organise into anticyclones. These conclusions are the same as arrived at in previous experimental investigations (albeit with significantly poorer resolution and accuracy) for cylinder wakes in homogeneous, rotating fluids [20-22]. The stabilising and destabilising effects of rotation on the cyclonic, and anticyclonic shear layers, respectively, are consistent with the weak absolute vorticity stretching mechanism when $\mathrm{Ro} \approx 2.5$, as described in a linear stability analysis and numerical simulations in [23-25]. Both the strong horizontal divergence fields and the more irregular vortex core distribution on the anticyclonic side support such an explanation. In the decaying wake flow, local Rossby numbers continue to decrease until $\mathrm{Ro} \leqslant 1$, and at later times a reorganisation of the anticyclones can be accounted for satisfactorily by an explanation that does not involve three-dimensional motion [26, 27]. The sense of the asymmetry is opposite to that

usually described in quasi-geostrophic (QG) models, but the initial conditions here have a significant three-dimensional component.

A full parametric study is beyond the scope of this paper, but the competing effects of stratification and rotation are conveniently expressed by f/N. A stabilising background density gradient can serve to increase both the energy and regularity in a decaying wake flow, which passes through a non-equilibrium phase (NEQ, where $2 \leqslant Nt \leqslant 50$), when conversion of potential to kinetic energy is associated with decreased kinetic energy decay rates in the wake. The timescale depends only on N (not on the initial Fr!), so as f/N increases, rotation can be increasingly effective in disrupting the usual wake reorganisation. At the higher values of $f/N \geqslant 0.15$, the wider range of vortex interactions in the late wake indirectly supports the original hypothesis that the three-dimensional structure and vortex topology have been modfied. More solid confirmation will require high-resolution, time-resolved, three-dimensional data during the NEQ regime, and such a measurement is not currently possible.

* * *

We would like to thank Dr. D. RENOUARD for his encouragement and support, and le Congrès de Mécanique à Grenoble for the *Stagiaire* award during September 1996 and July-August 1997. Including this work as part of a general study of stratified bluff-body wakes has been possible due to the continued support of ONR Grant # N00014-96-1-1001, administered by Dr. P. PURTELL.

REFERENCES

[1] LIGHTHILL M. J., *Internal waves and related initial-value problems*, *Dyn. Atmos. Ocean*, **23** (1996) 3-17.
[2] RILEY J. J., METCALFE R. W. and WEISSMAN M. A., *Direct numerical simulations of homogeneous turbulence in density stratified fluids*, in *Nonlinear Properties of Internal Waves*, edited by B. J. WEST (AIP) 1981, pp. 79-112.
[3] VOROPAYEV S. I., AFANASYEV Y. D. and FILIPPOV I. A., *Horizontal jets and vortex dipoles in a stratified fluid, J. Fluid Mech.*, **227** (1991) 543-566.
[4] VOROPAYEV S. I. and AFANASYEV Y. D., *Vortex Structures in a Stratified Fluid* (Chapman & Hall) 1994.
[5] FLÓR J. B. and VAN HEIJST G. J. F., *Experimental study of dipolar vortex structures in a stratified fluid*, *J. Fluid Mech.*, **279** (1994) 101-134.
[6] NIELSEN A. H., RASMUSSEN J. J. and SCHMIDT M. R., *Self-organization and coherent structures in plasmas and fluids, Phys. Scr.*, **63** (1996) 49-58.
[7] NIELSEN A. H. and RASMUSSEN J. J., *Formation and temporal evolution of the lamb dipole, Phys. Fluids*, **9** (1997) 982-991.
[8] FLÓR J. B. and VAN HEIJST G. J. F., *Stable and unstable monopolar vortices in a stratified fluid, J. Fluid Mech.*, **311** (1996) 257-287.
[9] BECKERS M., VERZICCO R., CLERCX H. J. H. and VAN HEIJST G. J. F., *The vertical structure of pancake-like vortices in a stratified fluid: experiments, theory and numerical simulations*, to be published in *J. Fluid Mech.*
[10] LIN J. T. and PAO Y. H., *Wakes in stratified fluids: a review, Annu. Rev. Fluid Mech.*, **11** (1979) 317-338.
[11] CHOMAZ J. M., BONNETON P. and HOPFINGER E. J. *The structure of the near wake of a sphere moving horizontally in a stratified fluid, J. Fluid Mech.*, **254** (1993) 1-21.

[12] SPEDDING G. R., BROWAND F. K. and FINCHAM A. M., *Turbulence, similarity scaling and vortex geometry in the wake of a sphere in a stably-stratified fluid, J. Fluid Mech.*, **314** (1996) 53-103.
[13] SPEDDING G. R., *The evolution of initially-turbulent bluff-body wakes at high internal Froude number, J. Fluid Mech.*, **337** (1997) 283-301.
[14] DRITSCHEL D. G. and DE LA TORRE JUÁREZ M., *The instability and breakdown of tall columnar vortices in a quasi-geostrophic fluid, J. Fluid Mech.*, **328** (1996) 129-160.
[15] DRITSCHEL D. G. and MACASKILL C., *On the numerical simulation of quasi-geostrophic turbulence, Phys. Fluids*, **11** (1999) 1512-1520.
[16] CHABERT D'HIERES G., DAVIES P. A. and DIDELLE H., *A laboratory study of the lift forces on a moving solid obstacle in a rotating fluid, Dyn. Atmos. Ocean*, **13** (1989) 47-75.
[17] CHABERT D'HIERES G., DAVIES P. A. and DIDELLE H., *Experimental studies of lift and drag forces upon cylindrical obstacles in homgeneous, rapidly rotating fluids, Dyn. Atmos. Ocean*, **15** (1990) 87-116.
[18] FINCHAM A. M. and SPEDDING G. R., *Low-cost, high-resolution DPIV for turbulent flows, Exp. Fluids*, **23** (1997) 449-462.
[19] SPEDDING G. R., BROWAND F. K. and FINCHAM A. M., *The long-time evolution of the initially-turbulent wake of a sphere in a stable stratification, Dyn. Atmos. Ocean*, **23** (1996) 171-182.
[20] BOYER D. L., KMETZ M., SMATHERS L., CHABERT D'HIERES G. and DIDELLE H., *Rotating open channel flow past right circular cylinders, Geophys. Astrophys. Fluid Dyn.*, **30** (1984) 271-304.
[21] TARBOURIECH L. and RENOUARD D., *Stabilisation et déstabilisation par la rotation d'un sillage plan turbulent, C. R. Acad. Sci. Paris, Sér. II*, **323** (1996) 391-396.
[22] TARBOURIECH L., *Dévelopment d'une méthode de vélocimétrie par images de particules pour les grandes dimensions - application à l'étude expérimentale d'un sillage turbulent soumis à la rotation*, PhD thesis, Equipe Coriolis, Institute de Mécanique de Fluides, Grenoble, France, 1996.
[23] LESIEUR M., YANASE S. and MÉTAIS O., *Stabilizing and destabilizing effects of a solid body rotation on quasi-two-dimensional shear layers, Phys. Fluids*, **3** (1991) 403-407.
[24] YANASE S., FLORES C., MÉTAIS O. and RILEY J. J., *Rotating free-shear flows, 1, Linear stability analysis, Phys. Fluids*, **5** (1993) 2725-2737.
[25] MÉTAIS O., FLORES C., YANASE S., RILEY J. J. and LESIEUR M., *Rotating free-shear flows, Part 2, Numerical simulation, J. Fluid Mech.*, **293** (1995) 47-80.
[26] JOHNSTON J. P., HALLEEN R. M. and LEZIUS D. K., *Effects of spanwise rotation on the structure of two-dimensional fully developed turbulent channel flow, J. Fluid Mech.*, **56** (1972) 533-557.
[27] TRITTON D. J., *Stabilization and destabilization of turbulent shear flow in a rotating fluid, J. Fluid Mech.*, **241** (1992) 503-523.